Supplementary Materials and Methods - Leithner et al.

Cell lines

The human cell lines NCI-H23 (H23, ATCC number CRL-5800), NCI-H358 (H358, CRL-5807), NCI-H441 (H441, HTB-174) and NCI-H1299 (H1299, CRL-5803) were purchased directly from American Type Culture Collection (ATCC, Manassas, VA). The human cell lines A549 (Cat. No. 300114), A427 (300111) and HepG2 (300198) were purchased directly from Cell Lines Service (Eppelheim, Germany). NCI-H460 cells (H460) were a kind gift from Martin P. Barr, Institute of Molecular Medicine, St. James's Hospital and Trinity College Dublin, Dublin, Ireland, to A.H. H23, H358, H441, H460 and H1299 cells were cultured in RPMI 1640 supplemented with 10% fetal calf serum (FCS, Biowest, Nuaillé, France) and antibiotics (further referred to as RPMI 1640 growth medium). A549 and A427 cells were cultured in DMEM-F12 medium (Gibco, Waltham, MA) supplemented with 10% FCS (Biowest) and antibiotics. HepG2 cells were grown in DMEM low glucose (Gibco) supplemented with 10% FCS and antibiotics. Mycoplasma tests were performed every three months. Cell lines authentication was done for all cell lines by Short Tandem Repeat (STR) analysis using the PowerPlex 16HS System (Promega, Madison, WI).

Stable isotopic labelling

Cells were plated in normal growth medium ($5x10^6$ cells per $75cm^2$ culture flask) and after 24 hours cells were washed two times with PBS. For stable isotopic labelling, A549 cells were incubated in glucose- and glutamine free, serum-free DMEM medium (Gibco) supplemented with different concentrations of D-glucose and $^{13}C_5$-glutamine (Sigma-Aldrich, St. Louis, MO) or $^{13}C_3$-lactate (Sigma-Aldrich). In the case of H23 cells, tracers were diluted in glucose-, glutamine-, arginine-, lysine-, and serum-free RPMI 1640 medium (RPMI SILAC, Gibco) supplemented with arginine and lysine at the concentrations present in normal RPMI 1640 medium. Isotopic labelling of lipids was performed for 24 to 72 hours (Scheme in SI

Appendix, Fig. S3*B*). Labelling of PEP, 2-PG, 3-PG, and glutamate, which were assumed to reach isotopic steady state early due to their rapid turnover and small pool size, was performed for 12 hours after 60 hours pre-treatment under the indicated conditions. In all experiments controls with unlabelled glutamine and lactate, applied at the same concentrations as the tracers, were included. Media were replaced every 24 h. Prior to sample extraction with methanol cells were briefly washed with glucose- and glutamine free medium.

Sample preparation for mass spectrometry

Lipid extraction was performed as described (1), with minor alterations: One to five million cells were homogenized in 1.5 ml methanol three times for 10 s with a sonicator and a rotor-stator homogenizer to disrupt the cell membranes. As extraction control 5 nmol of PC 24:0 were added and after addition of 2.5 ml methyl-*tert*-butyl ether (MTBE) the mixture was vortexed for 10 s and sonicated for 10 min. After further addition of 2.5 ml MTBE and 10 min overhead shaking, 1.25 ml of deionized water was added to induce phase separation. After further 10 min overhead shaking, the samples were centrifuged (3 min, 1350 g, 21°C) and the upper organic phase was recovered. The lower aqueous phase was re-extracted with 2 ml of the upper phase of MTBE/methanol/water (10/3/2.5, v/v/v). The upper phases were combined and evaporated in a vacuum centrifuge. The dried lipid film was resuspended in 1 ml of chloroform/methanol (1:1, v/v). For the analysis of PEP, 2-PG, 3-PG, and glutamate cell homogenates in methanol were mixed 10 min with 1 ml chloroform and 1 ml water. Metabolites in the aqueous phase were vacuum-dried, dissolved in 1 ml methanol and derivatized with 50 µl trimethylsilyldiazomethane (TMSD) for 20 min at 22°C. To stop the derivatization 50 µl of a mixture of acetic acid/methanol (1/4, v/v) was added. The mix was vacuum-dried under N_2-flow and resuspended in 100 µl acetonitrile/ water (90/10, v/v) for LC/MS analysis of methylated metabolites.

Hydrophilic interaction liquid chromatography/mass spectrometry (HILIC/MS) for the analysis of isotopic enrichment of GPL

Chromatography was modified after Triebl et al. (2). Separation was performed on a Phenomenex Kinetex HILIC column (2.1 mm x 100 mm, 2.6 µm) (Phenomenex, Aschaffenburg, Germany), thermostatted to 50°C in a Thermo Accela 1250 HPLC system (Thermo Fisher Scientific, Waltham, MA). Mobile phase A was deionized water containing 1% (v/v) 1 M aqueous ammonium formate and 0.1% (v/v) formic acid. Mobile phase B was acetonitrile/isopropanol (5/2, v/v) with the same additives. Gradient elution started at 95% mobile phase B and changed to 75% B over 10 minutes. The column was re-equilibrated for 8 min with 95% B. Flow rate was 250 µl/min and 2 µl of sample, thermostatted to 10°C were injected using full loop injection mode.

The Orbitrap Velos Pro mass spectrometer (Thermo Fisher Scientific) operated in negative ion mode in alternating full MS and tandem MS mode. Full scan spectra were acquired at a resolution setting of 30,000. Tandem mass spectra were acquired at a resolution setting of 7,500 and phospholipid classes were analyzed using HCD activation (normalized collision energy, 75; activation time, 0.1; FT first mass mode, fixed at *m/z* 100). For the first 3 min, PI molecular species were isolated (*m/z* 887.5 ± 75), for the next 3 min diacyl-PE (non-plasmalogen PE) and plasmalogen-PE molecular species (*m/z* 745.5 ± 75) and for the remainder of the gradient PC molecular species (*m/z* 804.5 ± 100). Xcalibur Quan Browser and Microsoft Excel were used for data processing. For each lipid class investigated (PI, PE and PC), two sets of fragment ions were monitored: One head group fragment ion containing glycerol and the other set not containing glycerol. For each set, the extracted ion chromatograms of five isotopologues (containing zero, one, two, three and four ^{13}C atoms, respectively) were integrated. See SI Appendix, Fig. S9 for chemical structures and exact *m/z* values of target fragment ions. Areas of the respective isotopologues were normalized to

the monoisotopic ion. Isotopologue abundance was corrected for the natural abundance of ^{13}C using IsoCor software (3).

Reversed phase liquid chromatographic (RPLC)/MS quantitative analysis of GPL

Quantitation of individual phospholipid species was essentially performed as described (4). Chromatographic separation was performed on a Waters (Waters, Milford, MA, USA) BEH C8 column (100 x 1 mm, 1.7 µm), thermostatted to 50°C in a Dionex Ultimate 3000 RS UHPLC system. Mobile phase A was deionized water containing 1% (v/v) of 1 M aqueous ammonium formate and 0.1% (v/v) of formic acid as additives. Mobile Phase B was a mixture of acetonitrile/isopropanol 5:2 (v/v) with the same additives. Gradient elution started at 50% mobile phase B, rising to 100% B over 40 min; 100% B were held for 10 min and the column was re-equilibrated with 50% B for 8 min before the next injection. The flow rate was 150 µl/min. Prior to analysis the storage solvent was replaced by the injection solvent 2-propanol/chloroform/methanol (90:5:5, v/v/v) and LIPID MAPS internal standards (Avanti Polar Lipids, Alabaster, AL) were added: 1-dodecanoyl-2-tridecanoyl-sn-glycero-3-phosphocholine and 1-dodecanoyl-2-tridecanoyl-sn-glycero-3-phosphoethanolamine, 2 µM; 1-dodecanoyl-2-tridecanoyl-sn-glycero-3-phospho-1'-myo-inositol ammonium salt, 1.5 µM. The samples were kept at 8°C and the injection volume was 2 µl.

The Orbitrap Velos Pro mass spectrometer (Thermo Fisher Scientific) was operated in Data Dependent Acquisition mode using a HESI II ion source. Every sample was measured once in positive polarity and once in negative polarity. Ion source parameters for positive polarity were as follows: source voltage: 4.5 kV; source temperature: 275°C; sheath gas: 25 arbitrary units; aux gas: 9 arbitrary units; sweep gas: 0 arbitrary units; capillary temperature: 300°C. Ion source parameters for negative ion mode were: source voltage: 3.8 kV; source temperature: 325°C; sheath gas: 30 arbitrary units; aux gas: 10 arbitrary units; sweep gas: 0 arbitrary units; capillary temperature: 300°C. Full scan profile spectra from *m/z* 400-1200 for

positive ion mode and from 400-1600 in negative ion mode were acquired in the Orbitrap mass analyzer at a resolution setting of 100,000. For MS/MS experiments, the 10 most abundant ions of the full scan spectrum were sequentially fragmented in the ion trap using He as collision gas (normalized collision energy: 50; isolation width: 1.5; activation Q: 0.2; activation time: 10) and centroid product spectra were collected. The exclusion time was set to 10 s. Data were processed using Lipid Data Analyzer, as previously described (5,6) and annotated according to the official LIPID MAPS shorthand nomenclature (7). Lipid molecular species contributing in sum less than 5% to the total amount of the respective lipid class were omitted from the analysis. PC, PE and PE plasmalogens were analyzed as protonated molecules and PI as deprotonated molecules. Lipids were quantified using the internal standard approach and a one-point calibration and normalized to the protein content in parallel samples of cells treated exactly in the same way as cells used for MS.

Gas chromatography/mass spectrometry (GC/MS) of free fatty acids

Aliquots of the lipid extracts (200 µl) were derivatized with pentafluorbenzyl bromide (PFBBr). After addition of 4 nmol of C15:0 as internal standard, the solvent was evaporated by nitrogen. Thereafter, 20 µl N,N-diisopropylethylamine, 5 µl PFBBr, and 95 µl acetonitrile were added, and following an incubation for 10 min at room temperature the solvent was evaporated by nitrogen. The sample was dissolved in 70 µl cyclohexane and analyzed by GC/MS. A 5977A GC/MSD (Agilent Technologies, Waldbronn, Germany), equipped with a TR-FAME 30 m column, was used in 1:10 split mode with 1 ml/min helium as carrier gas and 250°C injector temperature. The initial temperature of 150°C was held for 1 min, increased to 250°C at a rate of 10°C/min and the final temperature was held for 10 min. The mass spectrometer was operated in negative ion chemical ionization mode. Fatty acids were detected as carboxylates after in-source dissociation of the pentafluorobenzyl moiety using single ion monitoring. Methane was used as CI gas; source temperature was 250°C and transfer line temperature was 200°C. Relative quantitation was performed using Agilent

MassHunter and Microsoft Excel, by normalizing the peak areas of fatty acids to the signal of the C15:0 internal standard.

Liquid chromatography (LC)/MS for analysis of isotopic enrichment of PEP, 2-PG and 3-PG

Methylated species were separated on a Waters Acquity UPLC BEH Amide 2.1 x 150 mm; 1.7 µm column, thermostatted to 35°C in a Dionex Ultimate 3000 RS UHPLC system. Mobile phase A was a mixture of deionized water/acetonitrile 80:20 (v/v) containing 0.5% (v/v) of 1 M aqueous ammonium formate (final concentration 5 mM); mobile phase B was a mixture of deionized water/acetonitrile 10:90 (v/v) containing 0.5% (v/v) of 1 M aqueous ammonium formate (final concentration 5 mM). Gradient elution started at 100% mobile phase B and was held for 4 min, degrading to 37.5% B over 9.30 min, was held for 0.7 min; rising to 100% A over 0.1 min and was held for 2.4 min; and the column was re-equilibrated with 100% B for 6.5 min before the next injection. The binary gradient elution was performed at a flow rate of 150 µl/min, the autosampler tray was kept at 6°C and 5 µl of sample were injected. After chromatographic separation methylated analytes were analyzed by a TSQ Quantum Ultra (Thermo Fisher Scientific) triple quadrupole mass spectrometer in negative ESI mode. Ion source parameters were: Source voltage: 3.0 kV; source temperature: 300°C; sheath gas: 35 arbitrary units; aux gas: 10 arbitrary units; sweep gas: 0 arbitrary units; capillary temperature: 350°C. Methylated molecular species were analyzed using specific selected reaction monitoring (SRM) scans. Peak areas were calculated by Xcalibur Quan Browser for all detected species.

Liquid chromatography (LC)/MS for analysis of isotopic enrichment of glutamic acid (glutamate)

Methylated species were separated on a Waters Acquity UPLC BEH Amide 2.1 x 150 mm; 1.7 µm column, thermostatted at 40°C in a Dionex Vanquish UHPLC system from Thermo Fisher scientific. Mobile phase A was deionized water containing 0.1% (v/v) formic acid and

0.5% (v/v) of 1 M aqueous ammonium formate (final concentration 5 mM); mobile phase B was a mixture of deionized water/acetonitrile 10:90 (v/v) containing 0.1% (v/v) formic acid , and 0.5% (v/v) of 1 M aqueous ammonium formate (final concentration 5 mM). Gradient elution started at 90% mobile phase B and was held for 1 min, degrading to 25% B over 1 min, was held for 4 min; rising to 100% B over 0.1 min, and the column was re-equilibrated with 100% B for 3.9 min before the next injection. The binary gradient elution was performed at a flow rate of 150 µl/min, the autosampler tray was kept at 6°C and 5 µl of sample were injected. After chromatographic separation methylated analytes were analyzed by a Q Exactive Focus (Thermo Fisher Scientific) mass spectrometer in positive ESI mode. Ion source parameters were: Source voltage: 3.5 kV; aux gas temperature: 300°C; sheath gas: 35 arbitrary units; aux gas: 10 arbitrary units; sweep gas: 0 arbitrary units; capillary temperature: 250°C, and resolution settings of 70,000 at 200 m/z. Methylated molecular species were analyzed using exact m/z ratio (<5 ppm). Peak areas were calculated by Xcalibur Quan Browser for all detected species.

Quantitative real-time PCR (qPCR) primer sequences

Total RNA was extracted with the peqGOLD Total RNA Kit (VWR, Vienna, Austria). Total RNA (1 µg) was reverse transcribed in a final volume of 20 µl using the RevertAid H Minus First Strand cDNA Synthesis Kit (Thermo Fisher Scientific). Real-time PCR was performed using the LightCycler 480 (Roche, Vienna, Austria) and the QuantiFast SYBR PCR kit (Qiagen, Hilden, Germany). Primers used were: 5´-CATCCGAAAGCTCCCCAAGTA-3´ (forward strand) and 5´-TGGAAATCAGCTGGGGACATC-3´ (reverse strand) for human PEPCK-M (*PCK2*); 5´-TCTCTCATAGCGTGAAAGCTGG-3´ (forward strand) and 5´-GCAGACTGGTCCCCTAAACA-3´ (reverse strand) for glycerol kinase (*GK*); 5´-ATTGCCGACAGGATGCAGGAA-3´ (forward strand) and 5´-GCTGATCCACATCTGCTGGAA-3´ (reverse strand) for β-actin (*ACTB*). *ACTB* served as a reference gene, as it showed stable expression. The relative expression of the gene of interest compared with the reference gene (*ACTB*) was calculated as ΔΔCp. ΔCp was

calculated by subtracting the Cp number of the gene of interest from that of *ACTB*. ∆Cp-values of the control group were subtracted from ∆Cp-values of the treated group.

Western blot

Cells were lysed on ice in RIPA buffer (Sigma-Aldrich) containing protease inhibitors. Proteins (20 µg/lane) were separated by sodium dodecyl sulfate-polyacrylamide gel electrophoresis using the Mini-PROTEAN® electrophoresis unit (BioRad, Hercules, CA) and transferred to a PVDF membrane (BioRad). Immunodetection was performed with the following antibodies: mouse monoclonal antibody to PEPCK-M (Abcam, #77047), mouse monoclonal antibody to CHOP (Clone 9C8, Thermo Fisher Scientific), or mouse monoclonal antibody to β-actin (loading control; Santa Cruz Biotechnology, Santa Cruz, CA). Peroxidase activity was detected using chemiluminescence detection (SuperSignal West Pico Chemiluminescent Substrate, Thermo Fisher Scientific) or Amersham ECL Prime Western Blotting Detection Reagent (GE Healthcare, Chicago, IL).

shRNA-mediated silencing and rescue by shRNA-resistant PEPCK-M

For stable expression of PEPCK-M shRNA or non-silencing shRNA, H23 cells were transfected with different commercially available shRNA plasmids targeting PEPCK-M or a non-silencing control shRNA (Qiagen) followed by selection with 1 µg/ml puromycin (Sigma-Aldrich) for two weeks. Monoclonal subcultures expressing two different PEPCK-M shRNA constructs (#1 and #2) or control shRNA were generated and the clones with the highest level of knockdown compared to a pool of monoclonal subcelllines expressing control shRNA were used in further experiments. For cultivation of cells, puromycin was used at the maintenance concentration of 0.5 µg/ml. During the course of the experiments puromycin was omitted. The level of PEPCK-M silencing was determined using qPCR and Western blot. In order to demonstrate, that phenotypic changes by PEPCK-M shRNA expression were not caused by off-target effects, PEPCK-M expression was rescued in PEPCK-M-silenced cells using PEPCK-M cDNA constructs resistant to the specific shRNA. PEPCK-M cDNA cloned

into the pCMV6-AC expression vector (Origene, Rockville, MD) was mutated by site-directed mutagenesis (SDM) at three codons of the respective shRNA binding site, in a manner that the amino acid sequence was not altered. SDM was performed using suitable primer pairs at Eurofins Genomics (Ebersberg, Germany) and confirmed by sequencing (Eurofins Genomics). For mass spectrometry experiments cells were transfected with the vector or the mutant cDNA plasmid in 25 cm^2 culture flasks (1 µg/flask) two days before the initiation of the treatment using jetPRIME transfection reagent (Polyplus-transfection SA, Illkirch, France). The transfection mixture was removed after 24 hours. Since cells expressing PEPCK-M-shRNA1 showed very low cell numbers and morphological signs of cell death after transfection with either vector or mutant PEPCK-M and subsequent starvation, we omitted PEPCK-M-shRNA1 expressing cells from analysis and performed rescue experiments only with PEPCK-M-shRNA2 expressing cells.

Subcutaneous growth of xenotransplants in nude mice

All animal experiments were approved by the Austrian Federal Ministry of Science, Research and Economy. Male athymic nude mice (Hsd:Athymic Nude – *Foxn1^{nu}*) eight weeks of age and specific pathogen-free were obtained from Envigo (Horst, The Netherlands) and were allowed to acclimate to the animal facility for two weeks before initiation of the study. H23 cells expressing PEPCK-M shRNA (two different constructs) or control shRNA were injected subcutaneously into the right flank ($5x10^6$ cells/animal) of mice anesthetized with isoflurane. Altogether three experimental groups with eight animals per group were included in the experiments. Sample size was estimated according to similar previous studies conducted by A.H. No animal planned to use in the study and injected with tumor cells was excluded from analysis. Tumor size ($w^2 \times l \times 0.52$) measured by caliper and body weight were assessed twice a week by one of three different observers. Blinding of animals was not performed. All mice were kept in the experiment for the same duration (12 weeks), before exceeding a max. tumor diameter of 15 mm. Mice were sacrificed by cervical dislocation under isoflurane anesthesia. Tumors were isolated as a whole, different tumor parameters (weight, volume,

size and macroscopic appearance) were determined, and parts of the tumor were cryopreserved or fixed and paraffin-embedded. Skin at the injection site (approximately 2.5 cm^2) of all mice without extractable tumor was fixed and paraffin-embedded and serial sections were stained using hematoxylin-eosin (HE). Liver, lung, and brain of all animals were fixed and paraffin-embedded and the absence of metastases was confirmed by examination of HE stained sections (two per organ).

Proliferation and colony formation assays

For the assessment of cell numbers, cells were plated at 200,000/well into 6-well plates in duplicates. After 24 hours cells were washed twice with PBS and incubated in DMEM or RPMI media containing 2 mM glutamine, different concentrations of glucose, and different concentrations of dialyzed FCS. The medium was replaced daily. Viable cell numbers were counted after washing once with PBS and trypsinization using the TC20 Automated Cell Counter (Biorad). For the determination of colony forming capacity, H23 cells were plated in RPMI 1640 growth medium (RPMI 1640 supplemented with 10% FCS) at the indicated numbers into 6-well plates in triplicates. After 24 hours cells were washed two times with PBS and incubated in starvation medium or normal growth medium for two, three or seven days, as indicated, followed by a recovery period in RPMI 1640 growth medium. In rescue experiments, DOPE (Avanti Polar Lipids) or glycerol (Sigma) was added at different concentrations during a starvation period of three days as described in Results. In case of DOPE, the methanol (vehicle) concentration was set to 0.25% in all samples. Glutaminase inhibitor CB-839 (MedChemExpress, Sollentuna, Sweden) or DMSO (vehicle) were added one day after plating in starvation medium or normal growth medium for a duration of 72 h, followed by two weeks recovery in normal growth medium. At the end of the experiments cells were washed with PBS, fixed in methanol:acetic acid (3:1 v/v) and colonies were stained using 0.4% crystal violet. Colonies with at least 50 cells were counted and the total covered area was determined using the ColonyArea plugin and ImageJ software (http://imagej.nih.gov/ij) as described (8) with minor modifications.

References (Supplementary Materials and Methods)

1. Matyash V, Liebisch G, Kurzchalia TV, Shevchenko A, Schwudke D (2008) Lipid extraction by methyl-tert-butyl ether for high-throughput lipidomics. *J Lipid Res* 49(5):1137-1146.

2. Triebl A, et al. (2014) Quantitation of phosphatidic acid and lysophosphatidic acid molecular species using hydrophilic interaction liquid chromatography coupled to electrospray ionization high resolution mass spectrometry. *J Chromatogr A* 1347:104-110.

3. Millard P, Letisse F, Sokol S, Portais JC (2012) IsoCor: Correcting MS data in isotope labeling experiments. *Bioinformatics* 28(9):1294-1296.

4. Triebl A, Trotzmuller M, Hartler J, Stojakovic T, Kofeler HC (2017) Lipidomics by ultrahigh performance liquid chromatography-high resolution mass spectrometry and its application to complex biological samples. *J Chromatogr B Analyt Technol Biomed Life Sci* 1053:72-80.

5. Hartler J, et al. (2011) Lipid data analyzer: Unattended identification and quantitation of lipids in LC-MS data. *Bioinformatics* 27(4):572-577.

6. Hartler J, et al. (2017) Deciphering lipid structures based on platform-independent decision rules. *Nature Methods* 14(12):1171-1174.

7. Liebisch G, et al. (2013) Shorthand notation for lipid structures derived from mass spectrometry. *J Lipid Res* 54(6):1523-1530.

8. Guzman C, Bagga M, Kaur A, Westermarck J, Abankwa D (2014) ColonyArea: An ImageJ plugin to automatically quantify colony formation in clonogenic assays. *PLoS One* 9(3):e92444.

Supplementary Figure Legends

Figure S1. PEPCK-M protein and mRNA expression and proliferation in a panel of lung cancer cell lines under different microenvironmental conditions. (*A*) PEPCK-M expression in seven NSCLC cell lines after incubation in media containing different concentrations of glucose (0.2 mM or 10 mM) in the presence or absence of dialyzed fetal calf serum (dFCS) for 48 h. Left, densitometry data from immunoblots (a representative blot is shown in Fig. 1*A*) normalized to non-starvation conditions (10 mM glucose, 10% dFCS) from four experiments. Right, mRNA levels normalized to non-starvation conditions from four experiments. Data are shown as mean +/- SEM. (*B*) Cells were grown under starvation conditions (0.2 mM glucose, no serum) or non-starvation conditions (10 mM glucose, 10% dFCS) as in (*A*) with daily medium replacement. Viable cell numbers were assessed, after trypsinizing the cells, using a cell counter. Results are mean +/- SEM from four independent experiments. Group comparisons were performed with two-way ANOVA. Low glc, low (0.2 mM) glucose; high glc, high (10 mM) glucose.

Figure S2. Phospholipid levels and label transfer from glutamine to glutamate and fatty acids under starvation. (*A*) A549 cells were grown in serum-free medium containing different concentrations of glucose for 96 hours. Levels of GPL classes were measured using HILIC/MS. Data are shown as mean +/- SEM from three independent experiments. No significant differences were found. (*B*) A549 cells were grown in serum-free medium containing different concentrations of glucose and unlabeled glutamine for 60 hours followed by 1 mM $^{13}C_5$-glutamine for 12 hours. Glutamate mass isotopologues were measured. Only fully labelled glutamine normalized to the unlabeled form is shown to allow better comparability with 2-PG and 3-PG enrichment data shown in Fig. 2*D*. Data are mean +/- SEM from four independent experiments. *** $P < 0.001$ (one-way ANOVA with Dunnett posthoc analysis versus 0.2 mM glucose). (*C*) A549 cells were grown in serum-free medium containing 0.2 mM glucose and 1 mM $^{13}C_5$-glutamine exactly as described in Fig. 2*B*. Mass

distributions of PE-bound fatty acids were measured using mass spectrometry. PE 18:1, containing 18 unlabelled carbons and one double bond and PE 18:0 M+2, containing 16 unlabelled carbons, two ^{13}C and no double bond, possess nearly the same mass and were indistinguishable using the mass spectrometry method applied. The same applies to the higher isotopologues. Thus, both possible variants are displayed on the X-axis. Data are displayed relative to the abundance of PE 18:1 M+0 as mean +/- SEM from three independent experiments.

Figure S3. Label enrichment of glycerol-free control fragments and dynamics of glucose and lactate in cell media during starvation experiments. (*A*) Isotopologues of glycerol-free ion fragments of PE-headgroups after $^{13}C_5$-glutamine labelling at different time-intervals in 0.2 mM glucose measured in parallel to glucose-containing ion fragments shown in Fig. 2*B*. Data are mean +/- SEM from three independent experiments. * $P < 0.05$ (one-way ANOVA with Dunnett posthoc analysis versus 24 h). (*B*) Schematic showing the protocol for isotopic labelling of lipids. Glc, glucose; Gln, glutamine; $^{13}C_5$-Gln, $^{13}C_5$-glutamine; mc, medium change; MS, sampling for mass spectrometry. (*C*) Glucose concentrations in media supernatants of cells cultured exactly as in stable isotope experiments. Data are mean +/- SD from three independent experiments. (*D*) Lactate concentration in cell culture supernatants under different glucose concentrations. Data are shown as mean +/- SEM from three independent experiments.

Figure S4. Conversion of lactate to GPL-bound glycerol. (*A*) Metabolic pathway for the biosynthesis of glycerol phosphate from glutamine and lactate (glyceroneogenesis) via PEPCK (PEPCK-M). Lactate enters the pathway via pyruvate carboxylation. Glutamine enters the pathway via the TCA cycle after conversion to α-ketoglutarate (α-KG). Both pathways yield fully labelled glycerol (M+3). Consecutive passes through the TCA cycle lead to glycerol M+1 and M+2. Grey circles denote ^{13}C labelling from $^{13}C_3$-lactate after oxidation to pyruvate followed conversion to acetyl-CoA (AcCoA) and condensation with OAA. (*B*)

Isotopologue abundance of GPL-glycerol was measured in A549 or H23 cells incubated with 1 mM $^{13}C_5$-glutamine ($^{13}C_5$-Gln) in the presence or absence of 10 mM lactate (Lac) or with 10 mM $^{13}C_3$-lactate ($^{13}C_3$-Lac) in the presence of 1 mM glutamine in serum-free, low glucose (0.2 mM) medium. Data are mean +/- SEM from three independent experiments. One-way ANOVA with Bonferroni post-hoc analysis was performed for the comparison of different experimental groups, as indicated. * $P < 0.05$. (*C*) Summary of contributions from glutamine and lactate to the glycerol backbone. Calculation based on enrichment data from experiments shown in (*B*). Blue bars sum up the contribution of glutaminolysis to glycerol and represent the sum of relative isotopologue abundances of glycerol M+1, M+2 and M+3 from $^{13}C_5$-glutamine. Relative isotopologue abundance of glycerol M+3 from $^{13}C_3$-lactate is shown in green. Hatched bars are the sum of M+1 and M+2 glycerol isotopologues (relative abundances) from $^{13}C_3$-lactate which can either be derived from fully labelled pyruvate followed by pyruvate carboxylation and additional turns of the TCA cycle, or indicate entry of lactate to the TCA cycle as acetyl-CoA. In the second case there is no net contribution of carbons since two carbons are lost as CO_2 (grey circles in *A*). Data are mean +/- SEM from three independent experiments. AcCoA, acetyl-CoA; GAP, glyceraldehyde phosphate; DHAP, dihydroxyacetone phosphate; OAA, oxaloacetate; PC, phosphatidylcholine; PE, phosphatidylethanolamine; PI, phosphatidylinositol.

Figure S5. Glyceroneogenesis from glutamine and lactate provides the glycerol backbone of plasmalogens. (*A*) Metabolic pathway for the biosynthesis of the glycerol backbone of plasmalogens from glutamine and lactate via PEPCK (PEPCK-M). Filled circles denote ^{13}C-labelling. ^{13}C from lactate (green circles) or from glutamine (blue circles) appear in the DHAP-pool. While the glycerol backbone of classical GPL is synthesized from glycerol phosphate, the glycerol backbone of plasmalogens (a type of ether lipids) is synthesized directly by attaching acyl chains to DHAP. The fatty acid in *sn*-1 position is then replaced by a fatty alcohol in ether linkage. (*B*) Label enrichment of the glycerol backbone in specific classes of PE, PE 34:1 (PE carrying fatty acid chains with 34 carbons and one double bond)

and PE 36:2, and of plasmalogen PE (PE P-) 36:4 and PE P-38:6 after labelling with $^{13}C_5$-glutamine or $^{13}C_3$-lactate in serum-free, low glucose (0.2 mM) medium. Data are mean +/- SEM from three independent experiments. One-way ANOVA with Bonferroni post-hoc analysis was performed for the comparison of different experimental groups, as indicated. * $P < 0.05$. AcCoA, acetyl-CoA; GAP, glyceraldehyde phosphate; DHAP, dihydroxyacetone phosphate; PE, phosphatidylethanolamine.

Figure S6. PEPCK-M silencing reduces total levels of phosphatidylethanolamine (PE) but not PE plasmalogens or free fatty acids. *(A)* H23 cells stably expressing non-silencing shRNA (control shRNA, Ctrl-sh) or PEPCK-M shRNA (PEPCK-M-sh2) were grown in serum-free, low glucose (0.2 mM) medium for 96 hours and levels of GPL were assessed using RPLC. The five most abundant species are shown. Data are mean +/- SEM from five independent experiments. * $P < 0.05$, ** $P < 0.01$, *** $P < 0.001$ (one-way ANOVA with Dunnett posthoc analysis versus Ctrl-sh). (*B*) H23 cells stably expressing Ctrl-sh or PEPCK-M-sh2 were transfected with the empty pCMV6-AC vector (Ctrl-sh vect and PEPCK-sh2 vect) or PEPCK-M-sh2 resistant PEPCK-M (PEPCK-sh2 mt2). 48 hours after transfection cells were treated as described in (*A*). GPL levels were measured using RPLC. PE was the most severely reduced GPL class, overexpression of PEPCK-M abrogated the effect of PEPCK-M shRNA, albeit with a high degree of variability. Data are mean +/- SEM from four independent experiments. ** $P < 0.01$, n.s., not significant (two-sided Student´s t-test). (*C*) Expression levels of PEPCK-M in cells treated as in (*B*). (*D* and *E*) H23 Ctrl-sh or H23 cells expressing two different constructs of PEPCK-M shRNA (PEPCK-M-sh1 or PEPCK-M-sh2) were grown as described in (*A*). Total levels of PE plasmalogens (*D*) and total levels of free fatty acids (*E*) were assessed. (*D*) The five most abundant PE plasmalogen species are displayed on the left, the sum of all detectable PE plasmalogen species is shown on the right. (*D*, *E*) Data are mean +/- SEM from five independent experiments. * $P < 0.05$, ** $P < 0.01$ (one-way ANOVA with Dunnett posthoc analysis versus Ctrl-sh).

Figure S7. Inhibition of s.c. tumor growth by PEPCK-M silencing. (*A*) Photographs of mice and tumors 12 weeks after s.c. injection with H23 lung cancer cells expressing non-silencing shRNA (Ctrl-sh), PEPCK-M shRNA-1 or PEPCK-M shRNA-2. (*B*) Tumor size measured by caliper. The tumor volume was calculated as described in SI Materials and Methods. (*C*) Representative hematoxylin and eosin (HE) stained section of a tumor 12 weeks after s.c. injection of H23 cells expressing Ctrl-sh. In contrast, cells expressing PEPCK-M shRNA (PEPCK-M-sh1 or PEPCK-M-sh2) failed to form macroscopic tumors. On serial HE stained sections of the skin and subcutaneous tissue only microscopic, residual tumors were found (highlighted regions), or tumors were not detectable on serial sections. Scale bar low magnification: 200 µm, scale bar high magnification: 50 µm.

Figure S8. Colony formation under starvation is reduced by glutaminase inhibitor and PEPCK-M silencing and shows partial rescue by DOPE but not by (unphosphorylated) glycerol. (A) Effect of glutaminase inhibitor CB-839 treatment parallel to starvation or under non-starvation conditions for 72 hours on colony forming capacity. Results are mean +/- S.E.M. from three independent experiments. * $P < 0.05$, ** $P < 0.01$, *** $P < 0.01$ on one group *t*-test for the comparison of treated cells versus untreated cells (100%). (*B,C*) Colony forming capability of H23 cells expressing control shRNA or PEPCK-M shRNA (PEPCK-M-sh1 or PEPCK-M-sh2) treated with 0.2 mM glucose in serum-free medium for 72 hours in the presence or absence of DOPE (PE 36:2) (*B*) or glycerol, a cell-permeable precursor of glycerol-phosphate (*C*). (*B,C*) Data are mean +/- SEM from four independent experiments. Group comparisons were performed using two-sided, unpaired *t*-test. * $P < 0.05$, ** $P < 0.01$. (*D*) Glycerol kinase expression in H23 cells or HepG2 liver adenoma cells, assessed by qPCR. Its low expression might explain the lack of a rescue effect of glycerol on colony formation.

Figure S9. Phospholipid head group fragment ions differing only in the glycerol moiety generated during mass spectrometry of lipids. Structures and nominal *m/z* are shown. PC, phosphatidylcholine; PE, phosphatidylethanolamine; PI, phosphatidylinositol.

Fig. S1

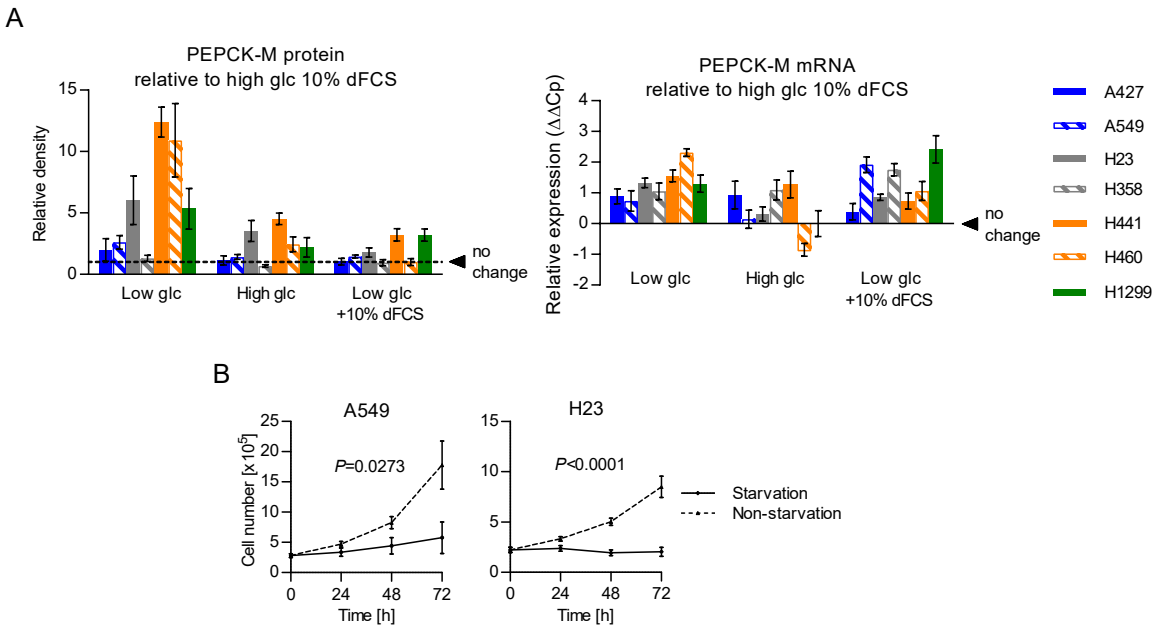
A
PEPCK-M protein
relative to high glc 10% dFCS
Relative density
15
10
5
0
Low glc
High glc
Low glc
+10% dFCS
no
change
PEPCK-M mRNA
relative to high glc 10% dFCS
Relative expression (ΔΔCp)
4
3
2
1
0
-1
-2
Low glc
High glc
Low glc
+10% dFCS
no
change
A427
A549
H23
H358
H441
H460
H1299
B
A549
P=0.0273
Cell number [x10^5]
25
20
15
10
5
0
0
24
48
72
Time [h]
H23
P<0.0001
15
10
5
0
0
24
48
72
Time [h]
Starvation
Non-starvation

Fig. S2

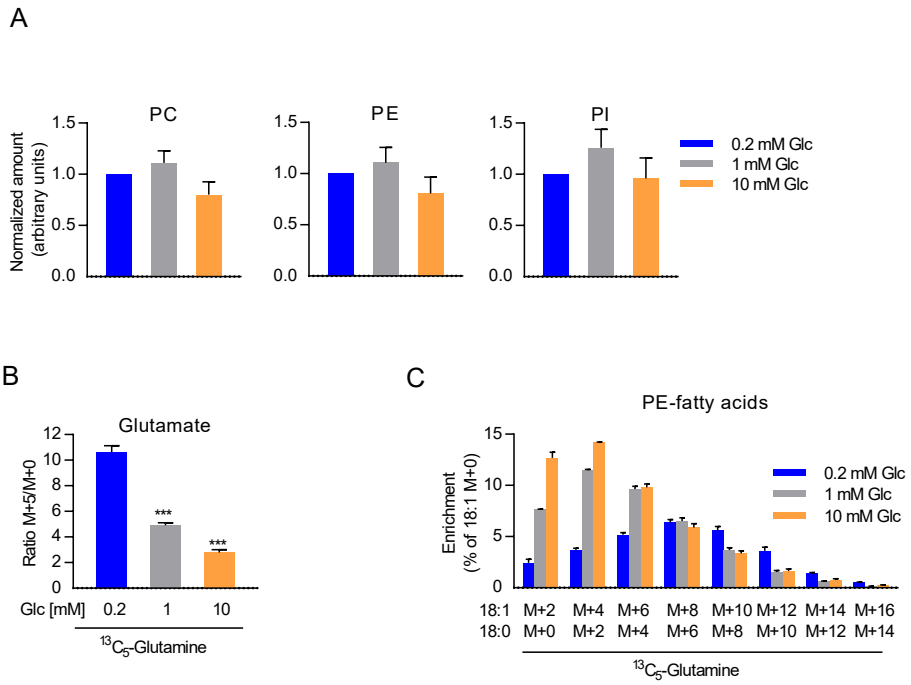
A
PC
PE
PI
Normalized amount (arbitrary units)
1.5
1.0
0.5
0.0
0.2 mM Glc
1 mM Glc
10 mM Glc
B
Glutamate
Ratio M+5/M+0
12
10
8
6
4
2
0
***
***
Glc [mM] 0.2 1 10
13C5-Glutamine
C
PE-fatty acids
Enrichment (% of 18:1 M+0)
15
10
5
0
0.2 mM Glc
1 mM Glc
10 mM Glc
18:1 M+2 M+4 M+6 M+8 M+10 M+12 M+14 M+16
18:0 M+0 M+2 M+4 M+6 M+8 M+10 M+12 M+14
13C5-Glutamine

Fig. S3

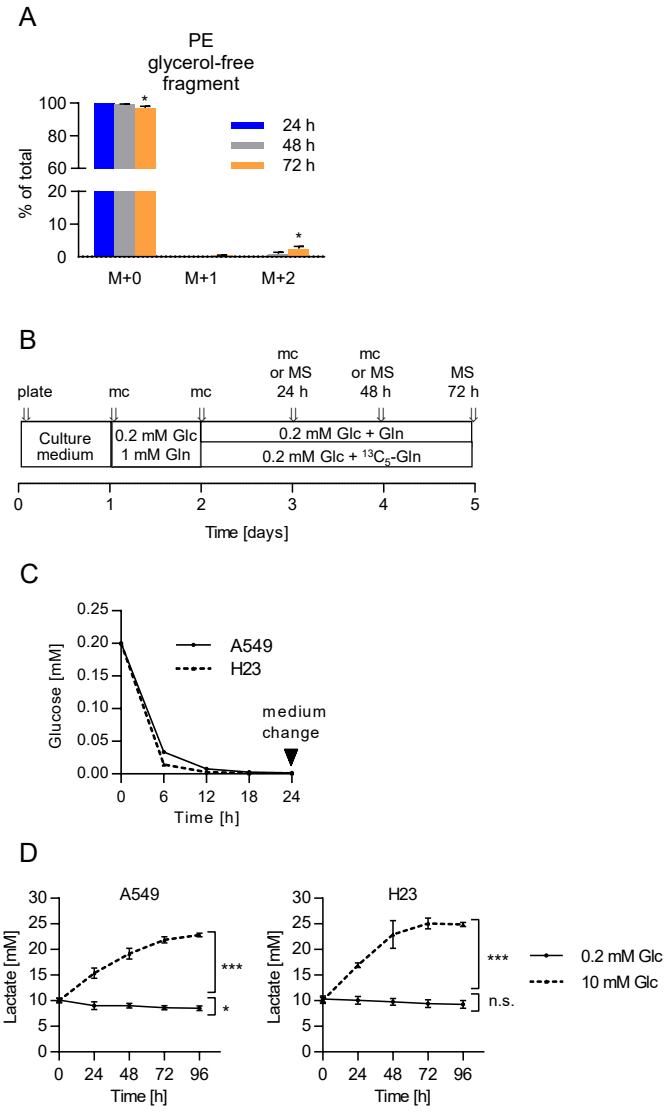
A
PE
glycerol-free
fragment
% of total
24 h
48 h
72 h
M+0
M+1
M+2
B
plate
mc
mc
mc
or MS
24 h
mc
or MS
48 h
MS
72 h
Culture
medium
0.2 mM Glc
1 mM Gln
0.2 mM Glc + Gln
0.2 mM Glc + 13C6-Gln
Time [days]
C
Glucose [mM]
A549
H23
medium
change
Time [h]
D
A549
H23
Lactate [mM]
***
*
n.s.
0.2 mM Glc
10 mM Glc
Time [h]

Fig. S4

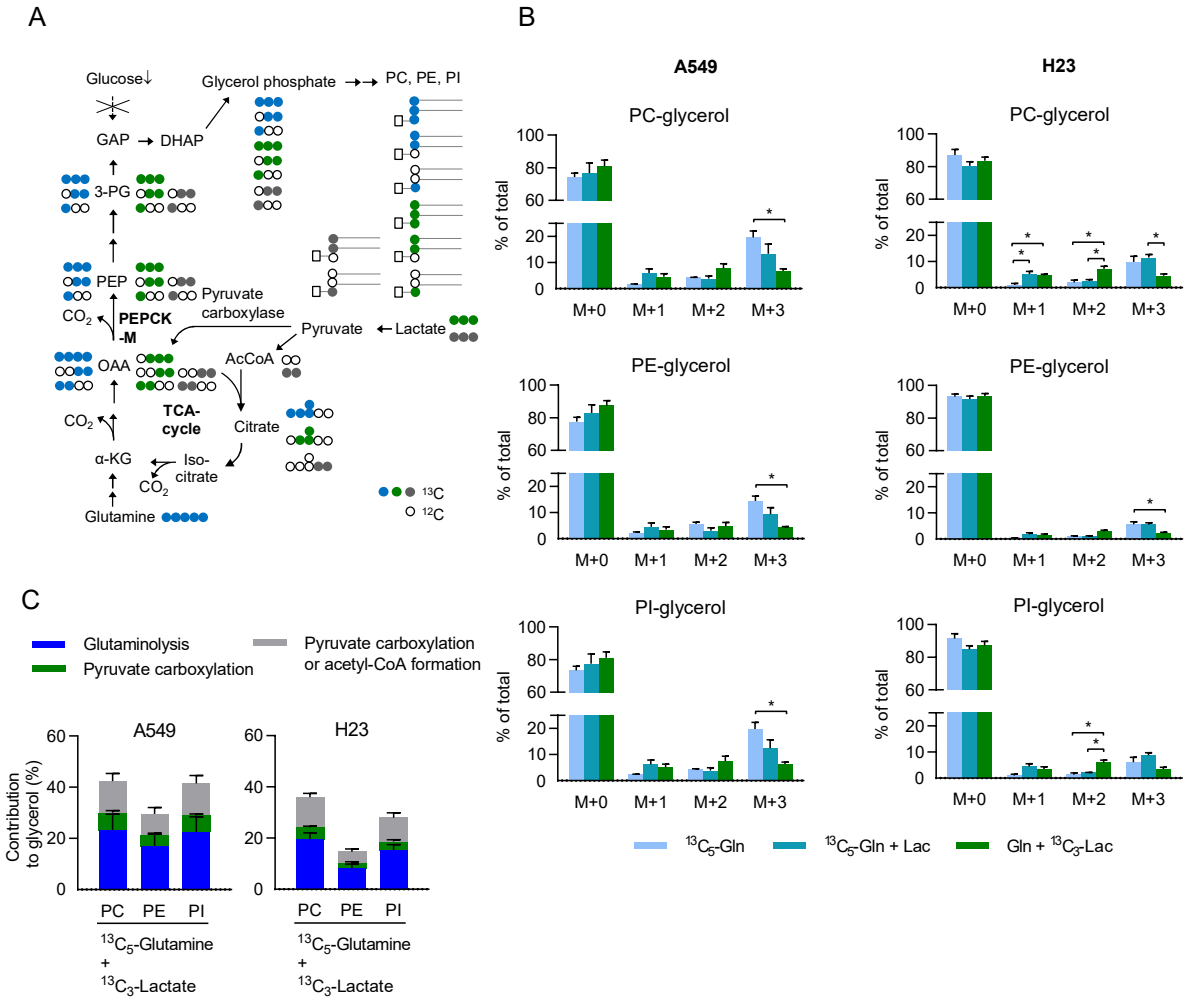
A
Glucose
Glycerol phosphate
PC, PE, PI
GAP
DHAP
3-PG
PEP
Pyruvate carboxylase
CO2
PEPCK -M
Pyruvate
Lactate
OAA
AcCoA
TCA-cycle
Citrate
α-KG
Iso-citrate
CO2
Glutamine
13C
12C
B
A549
H23
PC-glycerol
PE-glycerol
PI-glycerol
% of total
M+0
M+1
M+2
M+3
13C5-Gln
13C5-Gln + Lac
Gln + 13C3-Lac
C
Glutaminolysis
Pyruvate carboxylation
Pyruvate carboxylation or acetyl-CoA formation
A549
H23
Contribution to glycerol (%)
PC
PE
PI
13C5-Glutamine + 13C3-Lactate

Fig. S5

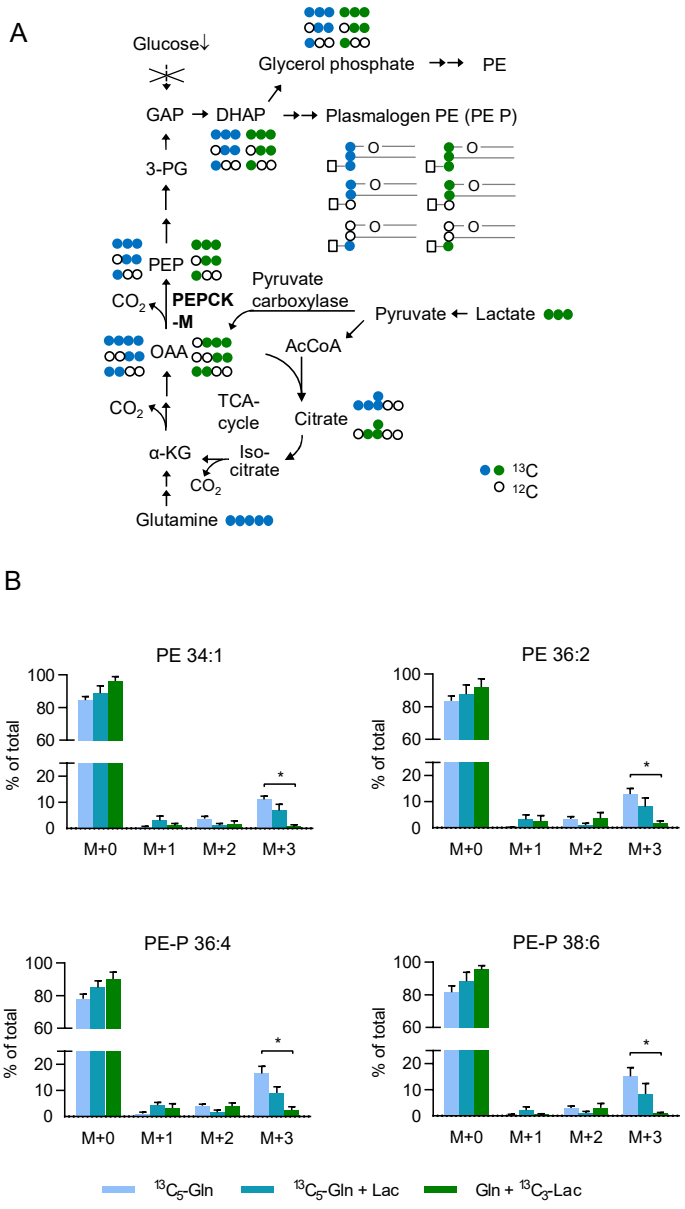
A
Glucose
Glycerol phosphate
PE
GAP
DHAP
Plasmalogen PE (PE P)
3-PG
PEP
PEPCK
-M
Pyruvate
carboxylase
Pyruvate
Lactate
AcCoA
OAA
TCA-
cycle
Citrate
α-KG
Iso-
citrate
Glutamine
13C
12C
B
PE 34:1
PE 36:2
PE-P 36:4
PE-P 38:6
% of total
M+0
M+1
M+2
M+3
13C5-Gln
13C5-Gln + Lac
Gln + 13C3-Lac

Fig. S6

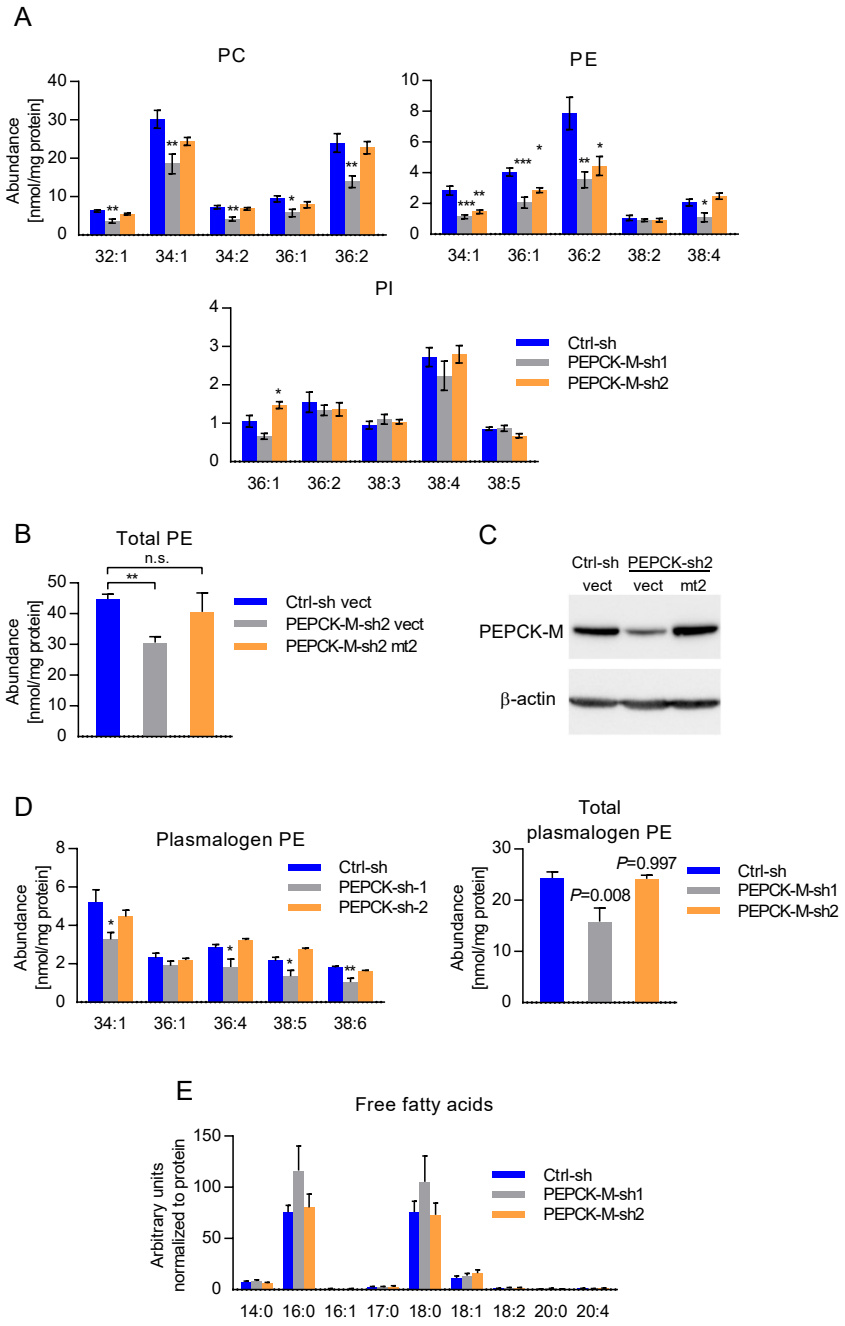
A
PC
PE
PI
Abundance [nmol/mg protein]
32:1
34:1
34:2
36:1
36:2
34:1
36:1
36:2
38:2
38:4
36:1
36:2
38:3
38:4
38:5
Ctrl-sh
PEPCK-M-sh1
PEPCK-M-sh2
B
Total PE
n.s.
Abundance [nmol/mg protein]
Ctrl-sh vect
PEPCK-M-sh2 vect
PEPCK-M-sh2 mt2
C
Ctrl-sh
PEPCK-sh2
vect
vect
mt2
PEPCK-M
β-actin
D
Plasmalogen PE
Abundance [nmol/mg protein]
Ctrl-sh
PEPCK-sh-1
PEPCK-sh-2
34:1
36:1
36:4
38:5
38:6
Total plasmalogen PE
P=0.997
P=0.008
Ctrl-sh
PEPCK-M-sh1
PEPCK-M-sh2
E
Free fatty acids
Arbitrary units normalized to protein
Ctrl-sh
PEPCK-M-sh1
PEPCK-M-sh2
14:0
16:0
16:1
17:0
18:0
18:1
18:2
20:0
20:4

Fig. S7

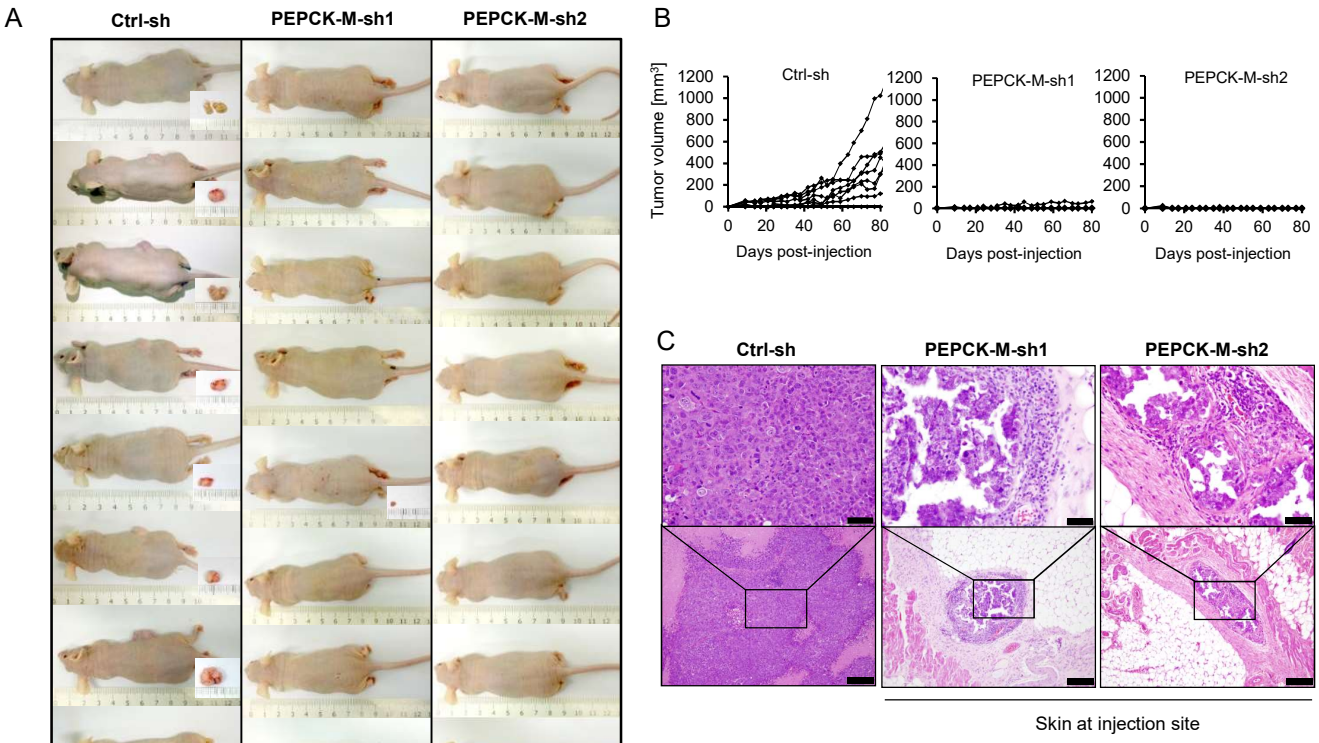
A
Ctrl-sh
PEPCK-M-sh1
PEPCK-M-sh2
B
Tumor volume [mm3]
Ctrl-sh
PEPCK-M-sh1
PEPCK-M-sh2
1200
1000
800
600
400
200
0
0 20 40 60 80
Days post-injection
C
Ctrl-sh
PEPCK-M-sh1
PEPCK-M-sh2
Skin at injection site

Fig. S8

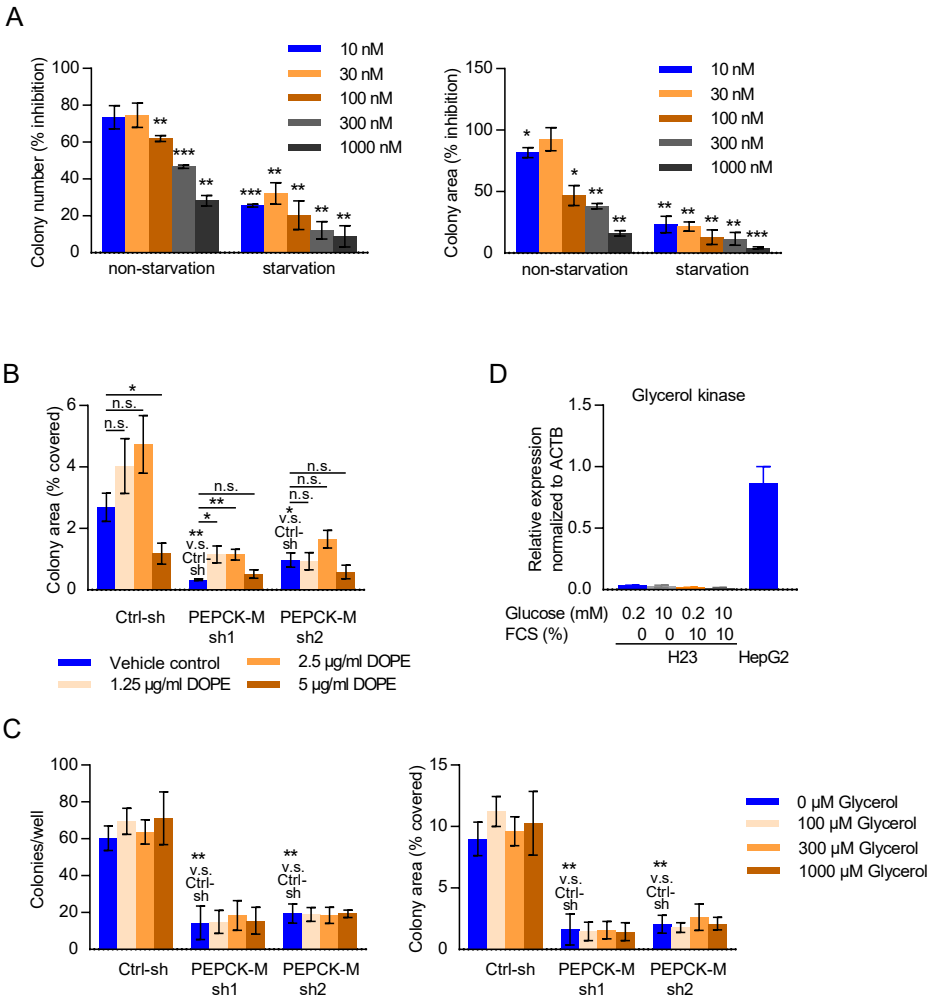
A
Colony number (% inhibition)
Colony area (% inhibition)
10 nM
30 nM
100 nM
300 nM
1000 nM
non-starvation
starvation
B
Colony area (% covered)
Ctrl-sh
PEPCK-M sh1
PEPCK-M sh2
Vehicle control
1.25 μg/ml DOPE
2.5 μg/ml DOPE
5 μg/ml DOPE
D
Glycerol kinase
Relative expression normalized to ACTB
Glucose (mM)
FCS (%)
H23
HepG2
C
Colonies/well
Colony area (% covered)
0 μM Glycerol
100 μM Glycerol
300 μM Glycerol
1000 μM Glycerol

Fig. S9

PC

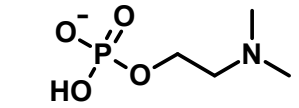

m/z 168

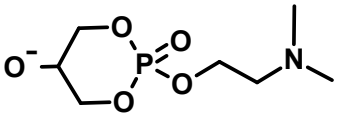

m/z 224

PE

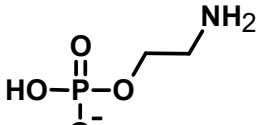

m/z 140

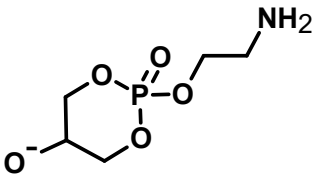

m/z 196

PI

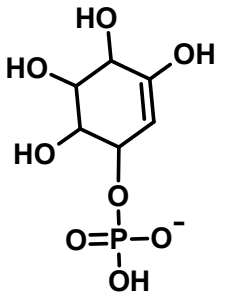

m/z 241

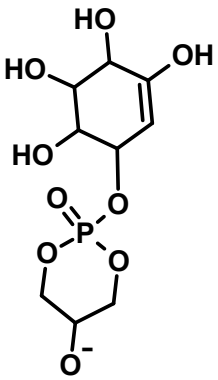

m/z 297